Vacuum polarization in supercritical fields and at frequencies above $2m$

J. I. Weise and D. B. Melrose
School of Physics, University of Sydney, NSW 2006, Australia
(Received 5 December 2005; published 7 February 2006)

The S-matrix form for the polarization tensor of the magnetized vacuum involves an integral over the parallel momentum, p_z, and a sum over the Landau levels of the virtual electrons and positrons. When the integrals over p_z are evaluated, they exhibit resonant-type behavior at each of the pair-creation thresholds. Emphasis is initially placed on the regime of soft photons, where simpler integrals are solved. When the sum is taken using the Euler-Maclaurin summation formula and the result is regularized, the known dispersive properties are reproduced for $\omega \ll m$. We evaluate the corrections of order ω^2 to these refractive indices and argue that they do not affect the known kinematic selection rules for photon splitting. With a simple modification to the low-frequency results, refractive indices are evaluated at frequencies up to just above the first pair-creation threshold, for supercritical magnetic fields.

DOI: 10.1103/PhysRevD.73.045005 PACS numbers: 12.20.−m, 41.20.Jb, 95.30.Cq, 97.60.Jd

I. INTRODUCTION

The effect of a magnetic field on the polarization of the vacuum was first derived by Weisskopf [1] using the Dirac hole theory and Heisenberg and Euler [2] via a Lagrangian technique. The theory was reviewed and extended by Erber [3] and Tsai and Erber [4]. A general derivation of the birefringence of the magnetized vacuum is based on an explicit expression for the vacuum polarization tensor. Two superficially very different forms are available: the Gehenian representation [5,6], also derived by Schwinger using the proper time technique [7], involves an integral over a combination of simple functions for arbitrary B; the S-matrix representation, involves generalized Laguerre polynomials with indices n, $n' = n - \nu$, where $n, n' = 0, 1, \ldots$, cf. [8]. The Gehenian form is the conventional basis for a derivation of the weak and strong field limiting forms of the indices of refraction [4].

Our purpose in this paper is to use the S-matrix form to extend results for the polarization of the magnetized vacuum from the known limits of soft photons, $\omega \ll m$ (we use natural units with $\hbar = c = 1$), and weak fields $B \ll B_{cr}$, with $B_{cr} = m^2/e = 4.4 \times 10^9$T the critical field. Two specific problems are of particular interest to us. The first problem is the fate of a photon with $\omega \gg m$ as it propagates away from the surface of a magnetar with $B \gg B_{cr}$. Assuming the photon is initially at a small angle, $\theta \ll 1$, to the magnetic field, the curvature of the field lines implies that θ increases along the propagation path. The first threshold for pair production is reached when the condition $\omega \sin\theta = 2m$ is satisfied. The relevant questions are whether the photon splits (into two photons) before reaching this threshold, and whether it decays into a pair on crossing the threshold. The other problem concerns the frequency dependence of the refractive indices, N. The S-matrix form allows one to separate the contributions to the dispersion into those from each of the resonances. In general, a resonance at $\omega = \omega_0$ contributes positively (negatively) to the dispersion at $\omega < \omega_0$ ($\omega > \omega_0$). The contribution to the refractive index then increases as the resonance is approached from below, decreases abruptly as the resonance is crossed and then continues to increase with increasing ω above the resonance. For the sequence of resonances at $n, n' = 0, 1, \ldots$, one expects $N - 1$ to exhibit this kind of behavior at each resonance. A corollary is that one expects the refractive index to asymptote to unity from below for $\omega \to \infty$. We treat the resonance at the first pair production threshold ($n' + n = 0$) explicitly, and show that it has a large effect on the refractive index of one mode but not the other. We comment on the resonances at $n + n' \geq 1$ but do not treat them in detail. As is well-known, for $\omega \ll m$, the refractive indices are greater than unity and independent of ω to a first approximation. We calculate the corrections of order ω^2 for $\omega \ll 2m$ and consider their possible implications for the kinematic constraints on photon splitting.

The S-matrix form has both conceptual and mathematical advantages for superstrong magnetic fields. The conceptual advantage is a straightforward physical interpretation in terms of resonances, providing a close analogy with the response tensor for a plasma. The contribution for given n, n' is related to one-photon pair creation with n, n' determining the energy eigenvalues, $\varepsilon_n(p_z) = (m^2 + p_z^2 + 2neB)^{1/2}$ and $\varepsilon_{n'}(p_z') = (m^2 + p_z'^2 + 2n'eB)^{1/2}$, of the electron and positron, with $k_z = \epsilon p_z - \epsilon' p_z'$ relating the components along $\mathbf{B}$ of the 3-momenta of the photon, the electron and the positron. The resonant part of the response tensor corresponds to one-photon pair annihilation and creation, with the resonance condition corresponding to conservation of energy, $\omega = \varepsilon_n(p_z) + \varepsilon_{n'}(p_z')$, where ω is the energy of the photon. The nonresonant part, which determines the refractive indices of the wave modes, corresponds to virtual pairs and may be determined from the resonant part by a dispersion relation [9,10]. A mathematical advantage arises from the way that the vacuum polarization tensor depends on its independent variables ω, $k_\perp$

and k_z. The contribution for each n, n' involves a resonance, which is determined by a p_z-integral over a resonant denominator that depends on ω and k_z but not $k_\perp$. All the $k_\perp$-dependence appears in the argument, $x = k_\perp^2/2eB = (k_\perp/m)^2/(2B/B_{cr})$, of functions related to Laguerre polynomials. On using the vacuum polarization tensor to evaluate the refractive indices, N, one writes $k_\perp = N\omega\sin\theta$ and $k_z = N\omega\cos\theta$ and then the resonances in the vacuum polarization tensor imply resonances in the refractive indices. One then has $x = (N\omega\sin\theta/m)^2/(2B/B_{cr})$, and the relation between the resonances in the vacuum polarization tensor and in the refractive indices is complicated by the functional form of the Laguerre polynomials. A major simplification occurs for $x \ll 1$, when only the leading term in an expansion in x dominates. Moreover, for $N \approx 1$, $x \ll 1$ is satisfied for any ω/m provided that B/B_{cr} is sufficiently large. This allows us to treat the resonance in the refractive indices at $n + n' = 0$ relatively simply for arbitrarily large B/B_{cr}.

The S-matrix form for the (unregularized) polarization tensor for a magnetized vacuum is written down in Sec. II, and it is projected onto its three physically allowed tensorial components. The integrals over p_z are evaluated with the imaginary parts reproducing the known absorption coefficients for pair creation [11]. Refractive indices for soft photons are derived to order ω^2 in Sec. III and are used to discuss Adler's [12] kinematic selection rules for photon splitting. The low-frequency results are extended in Sec. IV to give the refractive indices for frequencies just above the first pair-creation threshold for supercritical magnetic fields. In Sec. V, we discuss the effects that photon splitting and pair creation have on the gamma-ray spectra from the polar cap regions of highly magnetized pulsars. The results are discussed in Sec. VI.

II. THE S-MATRIX FORM FOR THE VACUUM RESPONSE TENSOR

The S-matrix form for the (unregularized) vacuum polarization tensor was written down by Melrose and Stoneham [8]. A first stage in regularizing involves projection onto a set of basis vectors, cf. Appendix A, with the nonphysical components discarded. This results in the three invariant components:

$$\alpha_i = -\frac{e^3 B}{(2\pi)^2}\int_{-\infty}^{+\infty} dp_z \sum_{n,n'} \frac{g_i}{[\omega^2 - (\varepsilon_n + \varepsilon'_{n'})^2]\varepsilon_n\varepsilon'_{n'}}, \quad (1)$$

with $\varepsilon_n = (m^2 + p_z^2 + p_n^2)^{1/2}$, $\varepsilon'_{n'} = (m^2 + p_z'^2 + p_{n'}^2)^{1/2}$, $p'_z = p_z - k_z$, $p_n^2 = 2neB$, $p_{n'}^2 = 2n'eB$, and

$$\begin{aligned}
g_0 &= -\frac{k^2}{k_\perp}\{\varepsilon'_{n'} p_n (J^{n-1}_{n'-n+1} J^n_{n'-n} + J^n_{n'-n-1} J^{n-1}_{n'-n}) \\
&\quad - \varepsilon_n p_{n'} (J^{n-1}_{n'-n+1} J^{n-1}_{n'-n} + J^n_{n'-n-1} J^n_{n'-n})\}, \\
g_1 &= \frac{k_\perp^2}{k^2} g_0 + 4(\varepsilon_n + \varepsilon'_{n'}) p_n p_{n'} J^{n-1}_{n'-n+1} J^n_{n'-n-1}, \\
g_2 &= -\frac{(\omega^2 - k_z^2)}{k^2} g_0 - \frac{(\omega^2 - k_z^2)}{k_z}(\varepsilon_n p'_z - \varepsilon'_{n'} p_z) \\
&\quad \times [(J^{n-1}_{n'-n})^2 + (J^n_{n'-n})^2].
\end{aligned} \quad (2)$$

The coordinate axes are defined by

$$\mathbf{B} = (0, 0, B), \qquad \mathbf{k} = (k_\perp\cos\psi, k_\perp\sin\psi, k_z), \quad (3)$$

with $\psi = 0$, and the J-functions are related to generalized Laguerre polynomials,

$$J^n_\nu(x) = (-)^\nu J^{n+\nu}_{-\nu}(x) = \left(\frac{n!}{(n+\nu)!}\right)^{1/2} e^{-x/2} x^{\nu/2} L^\nu_n(x),$$

with argument $x = k_\perp^2/2eB$. The next stage in the regularization involves removing a divergent term from α_0 and constant terms from $\alpha_1(k)$ and $\alpha_2(k)$. This is carried out by requiring $\mathrm{reg}\alpha_i|_{\mathbf{B}} = \alpha_i|_{\mathbf{B}} - \alpha_i|_{\mathbf{B}\to 0}$. (We apply the regularization to the Gehenian representation form in Appendix B.) There are three distinct integrals over p_z in (1) to evaluate:

$$\begin{aligned}
I^{(a)}_{nn'} &= \int_{-\infty}^{\infty} dp_z \frac{1}{[\omega^2 - (\varepsilon_n + \varepsilon'_{n'})^2]\varepsilon_n}, \\
I^{(b)}_{nn'} &= \int_{-\infty}^{\infty} dp_z \frac{1}{[\omega^2 - (\varepsilon_n + \varepsilon'_{n'})^2]\varepsilon'_{n'}}, \\
I^{(2)}_{nn'} &= \int_{-\infty}^{\infty} dp_z \left\{\frac{p'_z}{[\omega^2 - (\varepsilon_n + \varepsilon'_{n'})^2]\varepsilon'_{n'}} \right. \\
&\quad \left. - \frac{p_z}{[\omega^2 - (\varepsilon_n + \varepsilon'_{n'})^2]\varepsilon_n}\right\}.
\end{aligned} \quad (4)$$

There are three separate regions that need to be considered for each value of n, n': a region where gyromagnetic emission or absorption is kinematically allowed, a region where pair creation or annihilation is kinematically allowed, and a region where neither is allowed. Each integral has a different form in each of these three regions, and each needs to be analytically continued across the boundary between them. These regions are bounded by the zeros of the denominator in (4). It is convenient to write the denominator in the form

$$\frac{1}{\omega^2-(\varepsilon_n+\varepsilon'_{n'})^2} = -\frac{\omega'^2+\varepsilon_n^{02}-\varepsilon_{n'}^{02}+2p_zk_z-2\varepsilon_n(\varepsilon_n-\varepsilon'_{n'})}{4\omega'^2(p_z-k_zf_{nn'}-\omega g_{nn'})(p_z-k_zf_{nn'}+\omega g_{nn'})}, \tag{5}$$

$$f_{nn'}=\frac{\omega'^2+\varepsilon_n^{02}-\varepsilon_{n'}^{02}}{2\omega'^2}, \qquad g_{nn'}=\frac{[(\omega'^2+\varepsilon_n^{02}-\varepsilon_{n'}^{02})^2-4\omega'^2\varepsilon_n^{02}]^{1/2}}{2\omega'^2}, \tag{6}$$

with $\omega'^2=\omega^2-k_z^2$, $\varepsilon_n^{02}=m^2+2neB$ and $\varepsilon_{n'}^{02}=m^2+2n'eB$. The parameter $g_{nn'}$ is real when either gyromagnetic emission (or absorption) or pair creation (or annihilation) at given n, n' is possible, and imaginary when these are kinematically forbidden. A physical interpretation follows by writing the resonance conditions for these four processes in the form $\omega-\epsilon\varepsilon_n(p_z)+\epsilon'\varepsilon_{n'}(p'_z)=0$, $k_z-\epsilon p_z+\epsilon' p'_z=0$, with $\epsilon, \epsilon'=\pm1$. On solving these equations one finds

$$\begin{aligned}\epsilon p_{z\pm}&=k_zf_{nn'}\pm\omega g_{nn'},\\ \varepsilon_n(p_{z\pm})&=\omega f_{nn'}\pm k_zg_{nn'},\\ \epsilon' p'_{z\pm}&=k_z(\epsilon f_{nn'}-1)\pm\epsilon\omega g_{nn'},\\ \epsilon'\varepsilon_{n'}(p'_{z\pm})&=\omega(\epsilon f_{nn'}-1)\pm\epsilon k_zg_{nn'}.\end{aligned} \tag{7}$$

At the boundaries of the physically allowed regions one has $g_{nn'}=0$ corresponding to the pair-creation and gyromagnetic absorption thresholds $\omega'^2=(\varepsilon_n^0\pm\varepsilon_{n'}^0)^2$, respectively. The integrals are continuous across the gyromagnetic absorption thresholds but discontinuous across the pair-creation thresholds. The integrals in (4) are evaluated in Appendix C. Gyromagnetic absorption is not possible in the vacuum, but pair creation is possible, and is determined by the imaginary parts of the polarization tensor. The absorption coefficient for pair creation for each n, n' is evaluated in Appendix E using the imaginary parts of the integrals given in Appendix C and identities in Appendix D. The results reproduce those obtained by Daugherty and Harding [11]. The explicit expression that results for the real part of the vacuum response tensor, involving the real part of the integrals evaluated in Appendix C, still involves infinite sums over n and n', and the forms of the J-functions precludes any exact evaluation of the α_i. These sums converge rapidly if the argument of the J-functions is small, $x=k_\perp^2/2eB\ll1$. This condition is satisfied for all magnetic fields B for $\omega\ll m$ provided one has $k_\perp^2\lesssim eB/5$. This low-frequency limit is investigated in the next section. A simple modification to these low-frequency results provides solutions for frequencies up to just above the first pair-creation threshold ($n'=n=0$) for supercritical magnetic fields. This extension is discussed in Sec. IV.

III. LOW-FREQUENCY RESULTS

In this section we extend the known results for the refractive indices in the low-frequency limit, $\omega\ll m$, (e.g. [4,13]) to include the next higher order contributions in an expansion in ω. We then use these results to investigate whether they affect the kinematic selection rules for photon splitting.

A. Two low-frequency modes

The well-known (nondispersive) expressions for the refractive indices $N_\perp$ and $N_\parallel$ for the two vacuum modes are obtained by approximating the vacuum polarization tensor, described by the three invariants α_i, by an expansion in ω^2, and here we extend this expansion to order ω^4, corresponding to corrections of order ω^2 to the refractive indices. The resulting integrals over p_z were evaluated by [14]. The sums over n, n' reduce to a set of single sums over n, with only $n'=n, n\pm1, n\pm2$ contributing, and the sum over n is performed using the Euler-Maclaurin summation formula, viz.

$$\sum_{n=0}^{\infty}F_i(n)\simeq F_i(0)+F_i(1)+F_i(2)-\frac{1}{2}\{F_i(\infty)-F_i(3)\}+\frac{1}{12}\{F'_i(\infty)-F'(3)\}-\frac{1}{720}\{F'''(\infty)-F'''_i(3)\}+\int_3^\infty dnF_i(n), \tag{8}$$

with derivatives higher than the third neglected. The expressions for the α_i obtained in this way remain unregularized: notably α_0 has a divergent term of the form $\lim_{n\to\infty}\ln n$. Regularization of the α_i is achieved by subtracting the $B\to0$ limit, viz. $\mathrm{reg}\alpha_i|_B=\alpha_i|_B-\alpha_i|_0$, with

$$\alpha_0|_0=\frac{e^2k^2}{(2\pi)^2}\left\{\frac{1}{3}\lim_{n\to\infty}\ln(n)+\frac{1}{6}+\frac{(\omega^2-k_z^2)}{15m^2}-\frac{k_\perp^2}{15m^2}\right\}, \qquad \alpha_1|_0=\frac{e^2k_\perp^2}{(2\pi)^2}\frac{1}{6}, \qquad \alpha_2|_0=-\frac{e^2(\omega^2-k_z^2)}{(2\pi)^2}\frac{1}{6}. \tag{9}$$

The refractive indices of the two modes of the birefringent vacuum are labeled $\perp$ and $\parallel$ denoting whether the electric vector is along $\mathbf{k}\times\mathbf{B}$ or $\mathbf{k}\times(\mathbf{k}\times\mathbf{B})$ respectively. The symbol N is used to denote the refractive index rather than the traditional symbol n, which is used to label the Landau levels. These refractive indices are

$$N_\perp^2 = \frac{1+\chi_0}{1+\chi_0-\chi_1\sin^2\theta}, \qquad N_\parallel^2 = \frac{1+\chi_0+\chi_2}{1+\chi_0+\chi_2\cos^2\theta}, \tag{10}$$

$$\chi_0 \equiv \frac{4\pi\,\mathrm{reg}\alpha_0}{k^2} = \gamma_0 + \gamma_{01}(\omega^2-k_z^2)/m^2 + \gamma_{02}k_\perp^2/m^2,$$
$$\chi_1 \equiv \frac{4\pi\,\mathrm{reg}\alpha_1}{k_\perp^2} = \gamma_1 + \gamma_{11}(\omega^2-k_z^2)/m^2 + \gamma_{12}k_\perp^2/m^2,$$
$$\chi_2 \equiv \frac{4\pi\,\mathrm{reg}\alpha_2}{(\omega^2-k_z^2)} = \gamma_2 + \gamma_{21}(\omega^2-k_z^2)/m^2 + \gamma_{22}k_\perp^2/m^2, \tag{11}$$

with $k_z = N\omega\cos\theta$, $k_\perp = N\omega\sin\theta$. Explicit expressions for the variables γ_i and γ_{ij} are given in Appendix F. The χ_i in (10) have implicit dependences on the refractive indices through k_z^2 and $k_\perp^2$, and when these are expressed in terms of the refractive indices, one obtains quadratic equations in $N_\perp^2$ and $N_\parallel^2$, which are solved to find the refractive indices explicitly. The second derivatives with respect to frequency, $N''_{\perp,\parallel}$, are needed to discuss the kinematic restrictions on photon splitting, and these are written down in Appendix F.

B. Photon splitting

Below the pair-creation threshold, $\omega < 2m$, the only important loss mechanism for photons is photon splitting. The kinematic restrictions on photon splitting follow from the three-wave matching condition

$$N(\omega)\omega\hat{\mathbf{k}} - N(\omega_1)\omega_1\hat{\mathbf{k}}_1 - N(\omega_2)\omega_2\hat{\mathbf{k}}_2 = 0, \tag{12}$$

where variables without subscripts refer to the incoming photon and variables with subscripts 1 and 2 to the two outgoing photons. When the refractive indices are approximated by unity, the three photon propagation directions are the same (the three photons are collinear). When the small differences in the refractive indices from unity are taken into account, either the photon directions satisfy a triangle inequality for vector addition, or the splitting is forbidden. Adler [12] wrote the triangle inequality in the form

$$\Delta = \omega_1 N(\omega_1) + \omega_2 N(\omega_2) - (\omega_1+\omega_2)N(\omega_1+\omega_2) \geq 0, \tag{13}$$

and concluded that the only splitting that is both CP-invariant and kinematically allowed is $\perp\rightarrow\parallel\parallel$. The kinematic restrictions follow from (13) together with $N_\parallel(0) > N_\perp(0)$ and $N''_\perp(0)$, $N''_\parallel(0) > 0$. Only four splittings are consistent with CP-invariance, and of these, $N_\parallel > N_\perp$ excludes $\parallel\rightarrow\parallel\perp$ and $\parallel\rightarrow\perp\parallel$, and $N''_\perp(0) > 0$ excludes $\perp\rightarrow\perp\perp$.

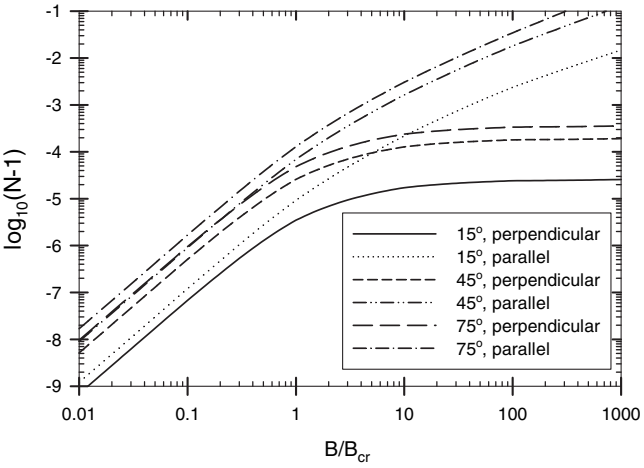

FIG. 1. Perpendicular and parallel refractive indices in the low-frequency limit ($\omega = 0.1m$) for a range of magnetic fields and angles θ.

The inclusion of the higher order terms in an expansion of the χ_i in ω^2 only slightly increases both refractive indices and their second derivatives ($N''_\perp, N''_\parallel > 0$) as B/B_{cr} and θ increase, with $N_\perp$ plateauing after $B/B_{cr} \sim 5$ and $N_\parallel$ continuing to increase (see Fig. 1). Adler's selection rules for photon splitting for nearly collinear photons remain unaltered with the only allowed splitting continuing to be $\perp\rightarrow\parallel\parallel$. A possible exception, which applies even without the inclusion of the higher order terms, is for strongly noncollinear propagation and for $B \lesssim 10B_{cr}$, due to $N_\perp$ at large angles exceeding $N_\parallel$ at small angles; for $N_\perp > N_\parallel$ in this sense the splitting $\perp\rightarrow\parallel\parallel$ is not allowed, and the splittings $\parallel\rightarrow\parallel\perp$ and $\parallel\rightarrow\perp\parallel$ are allowed. We have not explored the range of parameters where such strongly noncollinear splitting might occur, but it is clear that the phase space (if it is nonzero) is small and that such splittings cannot be of general importance in comparison with the nearly collinear case.

IV. EXTENSION TO HIGHER FREQUENCIES FOR SUPERCRITICAL FIELDS

A feature of the S-matrix expression for the vacuum polarization tensor is that it is simplified greatly when the power series expansion of the J-functions converges rapidly. This is the case for $k_\perp^2/2eB = N^2(\omega/m)^2 \times (B_{cr}/2B)\sin^2\theta \ll 1$, which is satisfied for $\omega > 2m$ in sufficiently strong fields, $B \gg B_{cr}$. The low-frequency results for $\mathrm{reg}\alpha_i$ can be used at higher frequencies if one does the following: first, the condition $k_\perp^2 \ll 2eB$ must be extended to include $\omega^2 \ll 2eB$ and $k_z^2 \ll 2eB$; and second, the low-

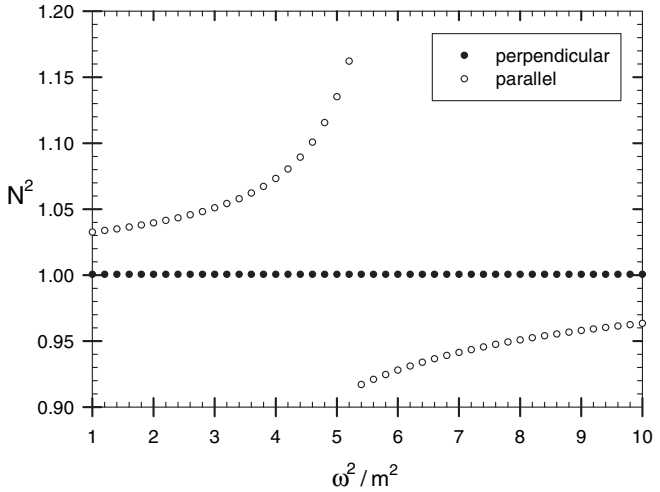

FIG. 2. Refractive indices squared for the two modes of the vacuum as a function of ω^2/m^2 from one up to $eB/5m^2$ in a magnetic field of $50B_{cr}$ and at an angle $\theta = 60°$. Refractive index values below $\omega^2/m^2 = 1$ do not differ significantly from those at one and agree with the low-frequency results when $\omega^2/m^2 \ll 1$.

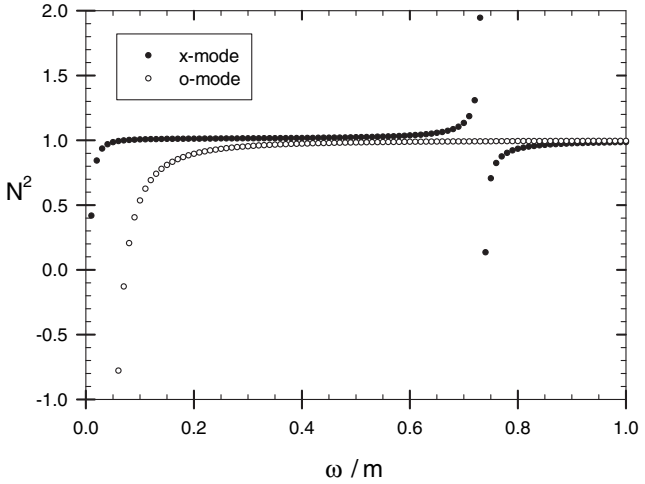

FIG. 3. Refractive indices squared for the two modes of a cold electron gas as a function of frequency ω in a magnetic field of B_{cr} and at an angle $\theta = 60°$.

frequency $n' = n = 0$ contribution, which only appears in $\mathrm{reg}\alpha_2$, must be replaced with its exact value, viz.

$$\frac{e^3B}{(2\pi)^2}\omega'^2\left(1-\frac{k_\perp^2}{2eB}\right)\left\{\frac{1}{3m^2}+\frac{\omega'^2}{15m^4}\right\}\Bigg|_{\omega\ll m} \longrightarrow \frac{e^3B}{(2\pi)^2}\frac{\omega'^2}{k_z}\left(1-\frac{k_\perp^2}{2eB}+\frac{k_\perp^4}{8e^2B^2}\right)I_{00}^{(2)}\Bigg|_{\text{arbitrary }\omega},$$

with $I_{00}^{(2)}$ given by (C1) or (C2) and $\omega'^2 = \omega^2 - k_z^2$.

Unlike the low-frequency case, the refractive indices cannot be evaluated exactly. Rather an iterative procedure is used with the refractive indices initially set to unity. More exact refractive indices are then calculated using (10). These values are then used in evaluating χ_i in the next iteration. Typically, convergence occurs after only four iterations except for $N_\parallel$ near the pair-creation threshold, where up to ten iterations are required. The results for the refractive indices for the two modes in a magnetic field of $50B_{cr}$ and at an angle $\theta = 60°$ are shown in Fig. 2 for $1 \le \omega^2/m^2 \le 10$.

As the first pair-creation threshold ($n' = n = 0$) is approached, $N_\parallel$ increases from $\sim$1.03 to $\sim$1.16 before dropping to $\sim$0.92 as the threshold is crossed, and then slowly increasing towards unity from below. This is similar to the behavior of the refractive indices of the two modes of a plasma. In Fig. 3, the refractive indices of the x- and o-modes of a cold electron gas are plotted against frequency (in units of m) for a magnetic field $B = B_{cr}$. As ω approaches the cyclotron frequency, $\omega_c = (m^2 + 2eB)^{1/2} - m$, the refractive index of the x-mode increases sharply while the o-mode remains nearly constant. As the resonance is crossed the refractive index of the x-mode drops to well below one thereafter increasing towards one from below. The behavior of the vacuum modes at the pair-creation threshold is similar, with $N_\parallel$ showing the resonant-like behavior, and $N_\perp$ remaining nearly constant. As the magnetic field increases the deviations of the parallel refractive index of the vacuum from unity become more pronounced (see Fig. 4 where two magnetic fields, $50B_{cr}$ and $100B_{cr}$ are compared). Above the $n' = n = 0$ pair-creation threshold, the parallel refractive index has real and imaginary components (see (C6)), with the real part N_r related to the dispersive properties of the vacuum and the

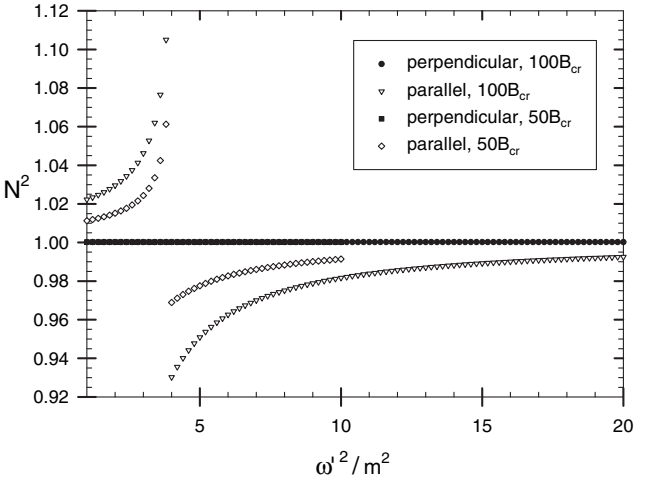

FIG. 4. Comparison of the refractive indices squared of the vacuum as a function of ω'^2 at two supercritical magnetic fields $100B_{cr}$ and $50B_{cr}$ and an angle $\theta = 30°$.

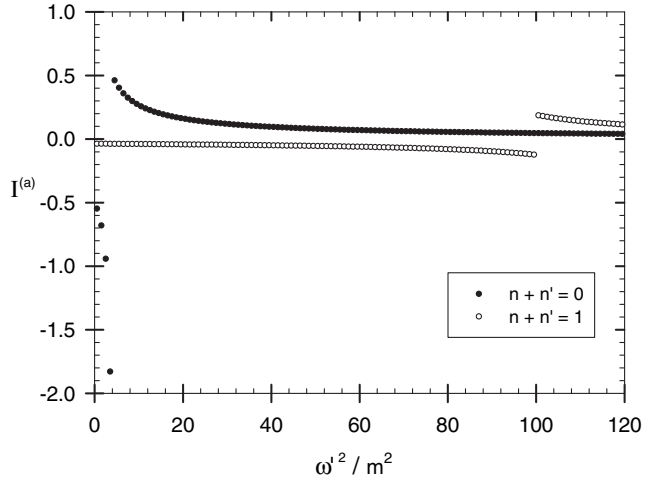

FIG. 5. The integral $I^{(a)}_{nn'}$ for $n + n' = 0, 1$ as a function of ω'^2 for a magnetic field of $50B_{cr}$ and arbitrary angle θ. The extent of the discontinuity at the pair-creation threshold decreases with increasing $n + n'$.

imaginary part N_i related to the absorption of photons into pair creation. The stronger the magnetic field, the greater the absorption. The deviation of N_r below unity is also larger for stronger magnetic fields.

An estimate of the magnetic field strength, B_r, at which N_r first drops below unity at the $n' = n = 0$ resonance can be found as follows. The real part of the integral $I^{(2)}_{00}$ at the first pair-creation threshold is given by $-4k_z/\omega'^2$ from which N_r can be evaluated at a given angle θ and a range of magnetic fields ($B \gg B_{cr}$). Extrapolating N_r back to unity, an estimate of B_r is obtained. For example, at an angle of $\theta = 30°$, this estimate is $B_r \sim 0.75$.

This resonantlike behavior occurs at each pair-creation threshold. This is evident in Fig. 5, where $I^{(a)}_{nn'}$ is plotted as a function of ω'^2 for the first two pair-creation thresholds, $n + n' = 0, 1$. As ω'^2 increases beyond $2m$, one would expect $N_\perp$ to remain fairly constant and $N_\parallel$ to continue to approach unity from below until the next pair-creation threshold ($n' + n = 1$) is approached. The behavior of $N_\perp$ at this threshold is similar to the behavior of $N_\parallel$ at the threshold $\omega = 2m$: specifically, $N_\perp$ increases and then drops to below unity as the threshold is crossed, and then approaches unity from below. The resonances at $n + n' = 0$ in $N_\parallel$ and at $n + n' = 1$ in $N_\perp$ are the first in an infinite sequence of resonances at $n + n' > 1$. The important qualitative difference between weak and strong fields is that these resonance overlap in the weak-field case, where they merge into a continuum, whereas they become well-separated and distinct in the strong-field case.

When $N_\parallel < N_\perp$, as is the case above $2m$, the kinematic selection rules for photon splitting are different from the low-frequency limit. Of the CP allowed splittings, the $\perp \rightarrow \parallel\parallel$ splitting is replaced by the $\parallel \rightarrow \parallel\perp$ and $\parallel \rightarrow \perp\parallel$ splittings. However, above the threshold for pair creation, photon splitting has to compete with pair creation, and can usually be neglected in comparison with it.

V. APPLICATION TO PULSARS

A specific motivation for our investigation of the vacuum polarization in strong fields and at high frequencies concerns pair creation in the magnetospheres of magnetars. In older versions of the polar cap model for pulsars [15], it was assumed that high-energy photons (energy ε_γ) are generated through curvature emission by primary electrons with Lorentz factors $\gamma \approx 10^7$. These photons are emitted nearly along the magnetic field lines ($\theta \lesssim 1/\gamma$) and are assumed to decay into pairs in high Landau levels when their angle of propagation, θ, increases such that the threshold $\varepsilon_\gamma \sin\theta > 2m$ is well satisfied. Subsequent models for pulsars developed this ''inner gap'' model further [16–18]. One effect of a relatively strong magnetic field is that the pairs are generated in the lowest possible Landau levels [19–21], which is $n = n' = 0$ for $\parallel$ -polarized photons and $n + n' = 1$ for $\perp$ -polarized photons. Thus the first threshold encountered for $\parallel$ -polarized photons is at $\varepsilon_\gamma \sin\theta = 2m$ ($n' = n = 0$), whereas the first threshold for $\perp$ -polarized photons at $\varepsilon_\gamma \sin\theta = m[1 + (1 + 2B/B_{cr})^{1/2}]$ ($n' + n = 1$) is much higher for $B \gg B_{cr}$. Another consequence of a stronger magnetic field is that photon splitting becomes more effective, and photons can split before they reach the threshold for pair creation. For the supercritical magnetic fields considered here, essentially all photons satisfying the threshold condition, $2m = \varepsilon_\gamma \sin\theta$ for $\parallel$ -polarized photon and $m[1 + (1 + 2B/B_{cr})^{1/2}] = \varepsilon_\gamma \sin\theta$ for $\perp$ -polarized photons, are absorbed once they reach the threshold for pair creation. The relevant question is whether or not they split before reaching the threshold. For $\parallel$ -polarized photons we find that

TABLE I. Distances in meters a photon of energy ε_γ in MeV (column 1) travels to acquire an ω satisfying $0.1m$ (column 2), $2m$ (column 3) and the $n' + n = 1$ pair-creation threshold (column 4 for $B_* = 50B_{cr}$ and column 6 for $B_* = B_{cr}$). The distances in meters to where the optical depth τ for photon splitting satisfies $\tau \gtrsim 1$ is given in columns 5 and 7 for B_* values of $50B_{cr}$ and B_{cr} respectively. The values of d_{01} and d_{ps} assume that the magnetic field (with strength B_* at the star's surface) decreases with distance as for a dipole at the center of the star, and B at the particular distance is given in parentheses.

ε_γ	$d_{0.1m}$	d_{2m}	$d_{01}(B)_{50}$	$d_{ps}(B)_{50}$	$d_{01}(B)_1$	$d_{ps}(B)_1$
10^4	1	20	109 (48.4)	4.9 (49.9)	27 (0.99)	10 (1.0)
10^3	10	200	975 (37.8)	33.8 (49.5)	270 (0.92)	69 (0.98)
10^2	100	2000	6030 (12.1)	237 (46.6)	2450 (0.52)	487 (0.87)
50	200	4000	9575 (6.7)	425 (44.1)	4565 (0.32)	925 (0.77)

Adler's selection rule precluding splitting continues to apply for supercritical fields, so that such photons (with $\varepsilon_\gamma > 2m$) are inevitably absorbed [13,22]. For the photon splitting process $\perp\rightarrow\parallel\parallel$ to be effective in preventing $\perp$ -polarized photons being absorbed, its optical depth τ must satisfy $\tau \gtrsim 1$ at a distance, denoted by d_{ps}, that is less than the distance at which pair creation would occur. The photon splitting attenuation coefficients have been estimated for frequencies $0.1 < \omega/m < 2$ [13,22–24]. Here we use values tabulated in Table II of [14] and assume photons are emitted initially parallel to a field line of a dipolar magnetic field. Although the attenuation coefficients (Table II of [14]) are for the low-frequency limit, we use them at higher frequencies where they lead to an underestimate [13,22], so that the distances we estimate represent upper limits.

In Table I we estimate the distances a $\perp$ -polarized photon propagates before $\varepsilon_\gamma \sin\theta$ reaches the values $0.1m$ (below which the low-frequency attenuation coefficients for photon splitting apply), $2m$ and $m[1 + (1 + 2B/B_{cr})^{1/2}]$ (its pair-creation threshold); these distances are denoted by $d_{0.1m}$, d_{2m} and d_{01} respectively. We present results for $B = 50B_{cr}$ and $B = B_{cr}$ and a range of ε_γ. The distance d_{01} varies substantially with B/B_{cr}, but $d_{0.1m}$ and d_{2m} do not. At $B = 50B_{cr}$, photon splitting is very effective in converting $\perp$ -polarized photons into $\parallel$ -polarized photons ($d_{ps} \ll d_{2m}$), and it remains effective at $B = B_{cr}$.

We conclude that the likely fate of high-energy photons emitted nearly along the field lines near the surface of a magnetar depends on their polarization: $\parallel$ -polarized photons propagate until they reach the pair-creation threshold at $\varepsilon_\gamma \sin\theta = 2m$ where they decay into a pair with $n = n' = 0$; $\perp$ -polarized photons split into two $\parallel$ -polarized photons, whose fate is the same as for photons with initially $\parallel$ -polarization. The only photons that can escape are those with sufficiently low ε_γ that pair creation cannot occur.

VI. DISCUSSION AND CONCLUSIONS

A particularly notable result of our investigation of the vacuum polarization at high frequencies in superstrong magnetic fields concerns the frequency dependence around each pair-creation threshold. It is well-known, e.g. [11], that there is a different threshold for different values, n, n', of the Landau levels of the created electron and positron, and that the absorption coefficient has a square-root singularity at each threshold. We find that the real part of the vacuum polarization tensor, and hence the refractive indices, exhibit resonancelike behavior at these thresholds: the contribution at the first threshold becomes large and positive as the threshold is approached from the lower-frequency side, and large and negative as it is approached from the high-frequency side. At subsequent thresholds, the refractive indices (now less than unity) decrease sharply thereafter slowly increasing towards unity from below. These resonances appear in refractive indices for the $\parallel$ -polarized mode for $n + n' \geq 0$ and in that for the $\perp$ -polarized mode for $n + n' \geq 1$. Whereas the refractive indices are greater than unity at low frequencies, the effect of this resonancelike behavior is that the refractive indices necessarily approach unity from below at arbitrarily high frequencies.

We consider how the frequency-dependences of the refractive indices affect the kinematic selection rules of Adler [12] for photon splitting, in particular, the corrections of order ω^2 in refractive indices as the first pair-creation threshold is approached from below. Adler found that the only splitting allowed in the low-frequency, weak dispersive limit, is $\perp\rightarrow\parallel\parallel$. We find that inclusion of the ω^2 corrections does not alter this qualitative conclusion. Hence, only $\perp$ -polarized photons can split, and they split into two $\parallel$ -polarized photons. If photon splitting is effective below the pair-creation threshold, all photons can become $\parallel$ -polarized before reaching the threshold $\varepsilon_\gamma \sin\theta = 2m$, where they can be absorbed, producing pairs in their ground states [19–21]. Such photon splitting has been invoked as an effective mechanism for photon conversion: Usov and Shabad [25] considered photon splitting as a means of producing $\parallel$ -polarized γ-rays and Harding, Baring and Gonthier [26] invoked photon splitting to explain the soft spectra of SGRs.

Our results allow discussions of the effect of the polarization of the vacuum on the propagation of high-frequency radiation through a magnetized plasma [27,28]. Existing studies are restricted to frequencies $\omega \ll m$, and with some more recent exceptions [29,30], only for magnetic fields $B \ll B_c$. A switching between plasma and vacuum dominated modes of the medium can modify the emission spectra of neutron stars, the more recent focus being the effect on the x-ray spectra of magnetars. The dispersive properties of the vacuum derived here may be regarded as a first step in treating the effects of the vacuum polarization on the propagation of γ-rays in highly magnetized neutron stars, magnetars.

APPENDIX A: CHOICE OF BASIS 4-VECTORS

The unregularized S-matrix form for the vacuum response tensor is given by [31]

$$\alpha^{\mu\nu}(k) = -\frac{e^3 B}{2\pi}\sum_{n,n'}\sum_{\epsilon'=\pm 1}\int\frac{dp_z}{2\pi}\int\frac{dp'_z}{2\pi}2\pi\delta[\epsilon'(p'_z + p_z) + k_z]\frac{\epsilon'[\omega - \epsilon'(\varepsilon_n + \varepsilon_{n'})]}{\omega^2 - (\varepsilon_n + \varepsilon_{n'})^2}[\Pi^{\epsilon'-\epsilon'}_{n'n}(\mathbf{k})]^{\mu\nu}. \quad \text{(A1)}$$

Since we are summing over the spin states, $[\Pi^{\epsilon'\epsilon}_{q'q}(\mathbf{k})]^{\mu\nu}$ is independent of the choice of spin operator; one may evaluate it by making any explicit choice of spin eigenstates. Choosing coordinate axes (3), explicit evaluation gives

$$
\begin{aligned}
2\varepsilon'_{n'}\varepsilon_n[\Pi^{\epsilon'\epsilon}_{n'n}(\mathbf{k})]^{00} &= (\varepsilon'_{n'}\varepsilon_n + p'_z p_z + \epsilon'\epsilon m^2)[(J^{n-1}_{n'-n})^2 + (J^{n}_{n'-n})^2] + 2\epsilon'\epsilon p_{n'} p_n J^{n-1}_{n'-n} J^{n}_{n'-n},\\
2\varepsilon'_{n'}\varepsilon_n[\Pi^{\epsilon'\epsilon}_{n'n}(\mathbf{k})]^{01} &= -\epsilon'\varepsilon_n p_{n'}[J^{n-1}_{n'-n} e^{i\psi} J^{n-1}_{n'-n+1} + J^{n}_{n'-n} e^{-i\psi} J^{n}_{n'-n-1}] - \epsilon\varepsilon'_{n'} p_n[J^{n}_{n'-n} e^{i\psi} J^{n-1}_{n'-n+1} + J^{n-1}_{n'-n} e^{-i\psi} J^{n}_{n'-n-1}],\\
2\varepsilon'_{n'}\varepsilon_n[\Pi^{\epsilon'\epsilon}_{n'n}(\mathbf{k})]^{02} &= i\epsilon'\varepsilon_n p_{n'}[J^{n-1}_{n'-n} e^{i\psi} J^{n-1}_{n'-n+1} - J^{n}_{n'-n} e^{-i\psi} J^{n}_{n'-n-1}] + i\epsilon\varepsilon'_{n'} p_n[J^{n}_{n'-n} e^{i\psi} J^{n-1}_{n'-n+1} - J^{n-1}_{n'-n} e^{-i\psi} J^{n}_{n'-n-1}],\\
2\varepsilon'_{n'}\varepsilon_n[\Pi^{\epsilon'\epsilon}_{n'n}(\mathbf{k})]^{03} &= (\varepsilon'_{n'} p_z + \varepsilon_n p'_z)[(J^{n-1}_{n'-n})^2 + (J^{n}_{n'-n})^2],\\
2\varepsilon'_{n'}\varepsilon_n[\Pi^{\epsilon'\epsilon}_{n'n}(\mathbf{k})]^{11} &= (\varepsilon'_{n'}\varepsilon_n - p'_z p_z - \epsilon'\epsilon m^2)[(J^{n-1}_{n'-n+1})^2 + (J^{n}_{n'-n-1})^2] + 2\epsilon'\epsilon p_{n'} p_n \cos(2\psi) J^{n-1}_{n'-n+1} J^{n}_{n'-n-1},\\
2\varepsilon'_{n'}\varepsilon_n[\Pi^{\epsilon'\epsilon}_{n'n}(\mathbf{k})]^{22} &= (\varepsilon'_{n'}\varepsilon_n - p'_z p_z - \epsilon'\epsilon m^2)[(J^{n-1}_{n'-n+1})^2 + (J^{n}_{n'-n-1})^2] - 2\epsilon'\epsilon p_{n'} p_n \cos(2\psi) J^{n-1}_{n'-n+1} J^{n}_{n'-n-1},\\
2\varepsilon'_{n'}\varepsilon_n[\Pi^{\epsilon'\epsilon}_{n'n}(\mathbf{k})]^{33} &= (\varepsilon'_{n'}\varepsilon_n + p'_z p_z - \epsilon'\epsilon m^2)[(J^{n-1}_{n'-n})^2 + (J^{n}_{n'-n})^2] - 2\epsilon'\epsilon p_{n'} p_n J^{n-1}_{n'-n} J^{n}_{n'-n},\\
2\varepsilon'_{n'}\varepsilon_n[\Pi^{\epsilon'\epsilon}_{n'n}(\mathbf{k})]^{12} &= -i(\varepsilon'_{n'}\varepsilon_n - p'_z p_z - \epsilon'\epsilon m^2)[(J^{n-1}_{n'-n+1})^2 - (J^{n}_{n'-n-1})^2] + 2\epsilon'\epsilon p_{n'} p_n \sin(2\psi) J^{n-1}_{n'-n+1} J^{n}_{n'-n-1},\\
2\varepsilon'_{n'}\varepsilon_n[\Pi^{\epsilon'\epsilon}_{n'n}(\mathbf{k})]^{13} &= -\epsilon' p_{n'} p_z[J^{n-1}_{n'-n} e^{-i\psi} J^{n-1}_{n'-n+1} + J^{n}_{n'-n} e^{i\psi} J^{n}_{n'-n-1}] - \epsilon p_n p'_z[J^{n}_{n'-n} e^{-i\psi} J^{n-1}_{n'-n+1} + J^{n-1}_{n'-n} e^{i\psi} J^{n}_{n'-n-1}],\\
2\varepsilon'_{n'}\varepsilon_n[\Pi^{\epsilon'\epsilon}_{n'n}(\mathbf{k})]^{23} &= -i\epsilon' p_{n'} p_z[J^{n-1}_{n'-n} e^{-i\psi} J^{n-1}_{n'-n+1} - J^{n}_{n'-n} e^{i\psi} J^{n}_{n'-n-1}] - i\epsilon p_n p'_z[J^{n}_{n'-n} e^{-i\psi} J^{n-1}_{n'-n+1} - J^{n-1}_{n'-n} e^{i\psi} J^{n}_{n'-n-1}].
\end{aligned}
\tag{A2}
$$

The tensor is Hermitian, and $[\Pi^{\epsilon'\epsilon}_{n'n}(\mathbf{k})]^{\mu\nu} = [\Pi^{\epsilon'\epsilon}_{n'n}(\mathbf{k})]^{*\nu\mu}$ determines the remaining terms in terms of those written in (A2). It is possible to construct four linearly independent 4-vectors from the available tensorial quantities, which include the wave 4-vector, k^μ, and the Maxwell tensor, $F^{\mu\nu}$, for the magnetostatic field. Writing $F^{\mu\nu} = Bf^{\mu\nu}$, $B = (\frac{1}{2}F^{\mu\nu}F_{\mu\nu})^{1/2}$, a possible choice was made by Shabad [32]

$$
\begin{aligned}
b_1^\mu &= (0, k_y, -k_x, 0), \qquad b_2^\mu = (k_z, 0, 0, \omega),\\
b_3^\mu &= \frac{k^2 g_\perp^{\mu\alpha} k_\alpha + k^\mu k_\perp^2}{k^2} = \frac{(\omega k_\perp^2, k_x\omega'^2, k_y\omega'^2, k_z k_\perp^2)}{k^2}.
\end{aligned}
\tag{A3}
$$

The vacuum polarization tensor can be described by (invariant) components along $b_i^\mu b_i^\nu$, with a null component along $b_4^\mu = k^\mu$ due to the charge-continuity and gauge-invariance conditions. We write

$$
\begin{aligned}
\alpha^{\mu\nu}(k) &= \sum_{i=0}^{2} \alpha_i(k) f_i^{\mu\nu},\\
f_0^{\mu\nu} &= \sum_{i=1}^{3} \frac{b_i^\mu b_i^\nu}{b_i^2} = g^{\mu\nu} - \frac{k^\mu k^\nu}{k^2},\\
f_i^{\mu\nu} &= \frac{b_i^\mu b_i^\nu}{b_i^2}.
\end{aligned}
\tag{A4}
$$

The vacuum response tensor is thereby described in terms of the three invariants $\alpha_i(k)$, $i = 0, 1, 2$.

APPENDIX B: REGULARIZATION IN THE GEHENIAN REPRESENTATION

The Gehenian representation gives (e.g., equation (32) of [33])

$$
\begin{aligned}
\alpha_i(k) &= \frac{e^2}{(2\pi)^2}\int_0^\infty \frac{d\alpha}{\alpha}\int_0^\alpha d\beta\,\gamma_i \exp\Big[-\alpha\frac{B_{cr}}{B}\\
&\quad + \frac{(\alpha^2-\beta^2)}{2\alpha}\frac{\omega^2 - k_z^2}{2eB} - \frac{\cosh\alpha - \cosh\beta}{\sinh\alpha}\frac{k_\perp^2}{2eB}\Big],\\
\gamma_0 &= \frac{\cosh\beta}{2\sinh\alpha}\Big(1 - \frac{\beta\tanh\beta}{\alpha\tanh\alpha}\Big)k^2,\\
\gamma_1 &= -\Big[\frac{\cosh\beta}{2\sinh\alpha}\Big(1 - \frac{\beta\tanh\beta}{\alpha\tanh\alpha}\Big) - \frac{\cosh\alpha - \cosh\beta}{\sinh^3\alpha}\Big]k_\perp^2,\\
\gamma_2 &= -\Big[\frac{\cosh\beta}{2\sinh\alpha}\Big(1 - \frac{\beta\tanh\beta}{\alpha\tanh\alpha}\Big) - \frac{\alpha^2-\beta^2}{2\alpha^2\tanh\alpha}\Big](\omega^2 - k_z^2).
\end{aligned}
\tag{B1}
$$

The resulting expressions for $\alpha_1(k)|_{\mathbf{B}}$ and $\alpha_2(k)|_{\mathbf{B}}$ are equivalent to equation (13) of [4] and equation (51) of [12]. These terms are not divergent, and regularizing them is trivial. The remaining term, $\alpha_0(k)|_{\mathbf{B}}$, is divergent and requires regularization to remove the divergence. For $k^2 \to 0$ one has

$$
\begin{aligned}
\alpha_0(k)|_{\mathbf{B},k^2\to 0} &= \frac{e^2k^2}{(2\pi)^2}\int_0^\infty \frac{d\alpha}{\alpha}\exp(-\alpha B_{cr}/B)\\
&\quad\times \int_0^\alpha d\beta \frac{\cosh\beta}{2\sinh\alpha}\Big[1 - \frac{\beta\tanh\beta}{\alpha\tanh\alpha}\Big].
\end{aligned}
\tag{B2}
$$

On evaluating the integral over β one obtains

$$
\begin{aligned}
\alpha_0(k)|_{\mathbf{B},k^2\to 0} &= \frac{e^2k^2}{2(2\pi)^2}\int_0^\infty \frac{d\alpha}{\alpha}\Big[-\mathrm{cosech}^2\alpha\\
&\quad + \frac{\coth\alpha}{\alpha}\Big]e^{-\alpha B_{cr}/B}.
\end{aligned}
\tag{B3}
$$

The limit $\mathbf{B} \to 0$ gives

$$
\alpha_0(k)|_{\mathbf{B}\to 0,k^2\to 0} = \frac{e^2k^2}{3(2\pi)^2}\int_0^\infty \frac{d\alpha}{\alpha}e^{-\alpha B_{cr}/B},
\tag{B4}
$$

which is divergent. The regularized form for $i = 0$ follows

by subtracting the divergent term (B4) from the general expression (B1).

APPENDIX C: EVALUATION OF p_z-INTEGRALS

The integrals (4) are evaluated first for $\omega'^2 < \omega'^2_{ga}$, $n' = n \pm a$ (a a positive integer), where $g_{nn'}$ is imaginary and the integrals are necessarily real. For simplicity in writing, in this section we omit the subscripts on $g_{nn'}$, $f_{nn'}$ and $f'_{nn'} = 1 - f_{nn'}$. Analytic continuation of the results into the region where g is real is trivial for $\omega'^2_{ga} < \omega'^2 < \omega'^2_{pp}$, where the integrals remain real; analytic continuation into the pair-creation region $\omega'^2 > \omega'^2_{pp}$ involves essentially only identifying the sign of the imaginary part that described the dissipation. The specific forms of the integrals depend not only on whether g is real or imaginary, but also on whether ω'^2 is less than, equal to or greater than $2aeB$: firstly, for $\omega'^2 < 2aeB$, one has $f < 0$, $f'(= 1 - f) > 0$ and $f' < 0$, $f > 0$ for $n' = n \pm a$ respectively; secondly, for $\omega'^2 = 2aeB$ ($\omega'^2_{ga} < 2aeB < \omega'^2_{pp}$), one has $f = 0$, $f' = 1$ and $f' = 0$, $f = 1$ for $n' = n \pm a$ respectively; and finally, for $\omega'^2 > 2aeB$, one has $f, f' > 0$ for both $n' = n \pm a$.

For $n' = n$ ($a = 0$, $\omega'^2_{ga} = 0$, $f = f' = \frac{1}{2}$), we find

$$I^{(a)}_{nn} = I^{(b)}_{nn} = \frac{1}{g_0\omega'^2}\left(\arctan(2g_0) - \frac{\pi}{2}\right),$$
$$I^{(2)}_{nn} = -\frac{2k_z}{\omega'^2}\left\{1 + \frac{2}{g_0}\left(\frac{1}{4} + g_0^2\right)\left(\arctan(2g_0) - \frac{\pi}{2}\right)\right\}, \tag{C1}$$

for g imaginary ($0 < \omega'^2 < \omega'^2_{pp}$) with $g_0 = (4\varepsilon_n^{02}/\omega'^2 - 1)^{1/2}$, and

$$I^{(a)}_{nn} = I^{(b)}_{nn} = \frac{1}{g\omega'^2}\left(\operatorname{arctanh}(2g) + \frac{i\pi}{2}\right),$$
$$I^{(2)}_{nn} = -\frac{2k_z}{\omega'^2}\left\{1 + \frac{2}{g}\left(\frac{1}{4} - g^2\right)\left[\operatorname{arctanh}(2g) + \frac{i\pi}{2}\right]\right\}, \tag{C2}$$

for g real ($\omega'^2 > \omega'^2_{pp}$) with $g = (1 - 4\varepsilon_n^{02}/\omega'^2)^{1/2}$. When $n' = n \pm a$ and g is imaginary, we find

$$I^{(a)}_{nn'} = -\frac{1}{\omega'^2}\ln\frac{\varepsilon^0_n}{\varepsilon^0_{n'}} + \frac{f'}{\omega'^2 g_0}\left\{\arctan\frac{g_0}{f} + \arctan\frac{g_0}{f'} - \pi\right\},$$
$$I^{(b)}_{nn'} = \frac{1}{\omega'^2}\ln\frac{\varepsilon^0_n}{\varepsilon^0_{n'}} + \frac{f}{\omega'^2 g_0}\left\{\arctan\frac{g_0}{f} + \arctan\frac{g_0}{f'} - \pi\right\},$$
$$I^{(2)}_{nn'} = -\frac{2k_z}{\omega'^2}\left\{1 + (f' - f)\ln\frac{\varepsilon^0_n}{\varepsilon^0_{n'}} + \frac{1}{g_0}(f'f + g_O^2)\right.$$
$$\left.\times\left(\arctan\frac{g_0}{f} + \arctan\frac{g_0}{f'} - \pi\right)\right\}, \tag{C3}$$

for $2aeB < \omega'^2 < \omega'^2_{pp}$, and

$$I^{(a)}_{nn'} = -\frac{1}{\omega'^2}\ln\frac{\varepsilon^0_n}{\varepsilon^0_{n'}} + \frac{f'}{\omega'^2 g_0}\left(\arctan\frac{g_0}{f} + \arctan\frac{g_0}{f'}\right),$$
$$I^{(b)}_{nn'} = \frac{1}{\omega'^2}\ln\frac{\varepsilon^0_n}{\varepsilon^0_{n'}} + \frac{f}{\omega'^2 g_0}\left(\arctan\frac{g_0}{f} + \arctan\frac{g_0}{f'}\right),$$
$$I^{(2)}_{nn'} = -\frac{2k_z}{\omega'^2}\left\{1 + (f' - f)\ln\frac{\varepsilon^0_n}{\varepsilon^0_{n'}} + \frac{1}{g_0}(f'f + g_O^2)\right.$$
$$\left.\times\left(\arctan\frac{g_0}{f} + \arctan\frac{g_0}{f'}\right)\right\}, \tag{C4}$$

for $\omega'^2_{ga} < \omega'^2 < 2aeB$ where

$$g_0 = \frac{[4\omega'^2\varepsilon_n^{02} - (\omega'^2 \mp 2aeB)^2]^{1/2}}{2\omega'^2},$$
$$f = \frac{(\omega'^2 \mp 2aeB)}{2\omega'^2}, \qquad f' = 1 - f,$$

for $n' = n \pm a$ respectively. For g real, whereby $\omega'^2 < \omega'^2_{ga}$ or $\omega'^2 > \omega'^2_{pp}$, we find

$$I^{(a)}_{nn'} = -\frac{1}{\omega'^2}\ln\frac{\varepsilon^0_n}{\varepsilon^0_{n'}} + \frac{f'}{\omega'^2 g}\left(\operatorname{arctanh}\frac{g}{f} + \operatorname{arctanh}\frac{g}{f'}\right),$$
$$I^{(b)}_{nn'} = \frac{1}{\omega'^2}\ln\frac{\varepsilon^0_n}{\varepsilon^0_{n'}} + \frac{f}{\omega'^2 g}\left(\operatorname{arctanh}\frac{g}{f} + \operatorname{arctanh}\frac{g}{f'}\right),$$
$$I^{(2)}_{nn'} = -\frac{2k_z}{\omega'^2}\left\{1 + (f' - f)\ln\frac{\varepsilon^0_n}{\varepsilon^0_{n'}} + \frac{1}{g}(f'f - g^2)\right.$$
$$\left.\times\left(\operatorname{arctanh}\frac{g}{f} + \operatorname{arctanh}\frac{g}{f'}\right)\right\}, \tag{C5}$$

for $\omega'^2 < \omega'^2_{ga}$, and

$$I^{(a)}_{nn'} = -\frac{1}{\omega'^2}\ln\frac{\varepsilon^0_n}{\varepsilon^0_{n'}} + \frac{f'}{\omega'^2 g}\left(i\pi + \operatorname{arctanh}\frac{g}{f} + \operatorname{arctanh}\frac{g}{f'}\right),$$
$$I^{(b)}_{nn'} = \frac{1}{\omega'^2}\ln\frac{\varepsilon^0_n}{\varepsilon^0_{n'}} + \frac{f}{\omega'^2 g}\left(i\pi + \operatorname{arctanh}\frac{g}{f} + \operatorname{arctanh}\frac{g}{f'}\right),$$
$$I^{(2)}_{nn'} = -\frac{2k_z}{\omega'^2}\left\{1 + (f' - f)\ln\frac{\varepsilon^0_n}{\varepsilon^0_{n'}} + \frac{1}{g}(f'f - g^2)\right.$$
$$\left.\times\left(i\pi + \operatorname{arctanh}\frac{g}{f} + \operatorname{arctanh}\frac{g}{f'}\right)\right\}, \tag{C6}$$

for $\omega'^2 > \omega'^2_{pp}$, where

$$g = \frac{[(\omega'^2 \mp 2aeB)^2 - 4\omega'^2\varepsilon_n^{02}]^{1/2}}{2\omega'^2},$$
$$f = \frac{(\omega'^2 \mp 2aeB)}{2\omega'^2}, \qquad f' = 1 - f,$$

for $n' = n \pm a$ respectively.

APPENDIX D: PRODUCTS OF J-FUNCTIONS

All the products of J-functions that appear in the S-matrix form of the vacuum polarization tensor may be

written in terms of two combinations: $[J^{n-1}_{n'-n}(x)]^2 + [J^{n}_{n'-n}(x)]^2$ and $J^{n-1}_{n'-n}(x)J^{n}_{n'-n}(x)$. The relevant relations are implied by the recursion formulas

$$x^{1/2}J^{n-1}_{\nu+1}(x) = (n+\nu)^{1/2}J^{n-1}_{\nu}(x) - n^{1/2}J^{n}_{\nu}(x), \tag{D1}$$

$$x^{1/2}J^{n}_{\nu-1}(x) = -n^{1/2}J^{n-1}_{\nu}(x) + (n+\nu)^{1/2}J^{n}_{\nu}(x). \tag{D2}$$

With $x = k_\perp^2/2eB$, $p_n = (2neB)^{1/2}$, the following identities are implied:

$$\begin{aligned}
k_\perp^2\{[J^{n-1}_{n'-n+1}(x)]^2 + [J^{n}_{n'-n-1}(x)]^2\} &= (p^2_{n'} + p^2_n)\{[J^{n-1}_{n'-n}(x)]^2 + [J^{n}_{n'-n}(x)]^2\} - 4p_{n'}p_nJ^{n-1}_{n'-n}(x)J^{n}_{n'-n}(x),\\
k_\perp^2 J^{n-1}_{n'-n+1}(x)J^{n}_{n'-n-1}(x) &= -p_{n'}p_n\{[J^{n-1}_{n'-n}(x)]^2 + [J^{n}_{n'-n}(x)]^2\} + (p^2_{n'} + p^2_n)J^{n-1}_{n'-n}(x)J^{n}_{n'-n}(x),\\
(p^2_{n'} - p^2_n)^2\{[J^{n-1}_{n'-n}(x)]^2 + [J^{n}_{n'-n}(x)]^2\} &= k_\perp^2(p^2_{n'} + p^2_n)\{[J^{n-1}_{n'-n+1}(x)]^2 + [J^{n}_{n'-n-1}(x)]^2\}\\
&\quad + 4k_\perp^2 p_{n'}p_nJ^{n-1}_{n'-n+1}(x)J^{n}_{n'-n-1}(x),\\
k_\perp\{J^{n-1}_{n'-n}(x)J^{n-1}_{n'-n+1}(x) + J^{n}_{n'-n}(x)J^{n}_{n'-n-1}(x)\} &= p_{n'}\{[J^{n-1}_{n'-n}(x)]^2 + [J^{n}_{n'-n}(x)]^2\} - 2p_nJ^{n-1}_{n'-n}(x)J^{n}_{n'-n}(x),\\
k_\perp\{J^{n}_{n'-n}(x)J^{n-1}_{n'-n+1}(x) + J^{n-1}_{n'-n}(x)J^{n}_{n'-n-1}(x)\} &= -p_n\{[J^{n-1}_{n'-n}(x)]^2 + [J^{n}_{n'-n}(x)]^2\} + 2p_{n'}J^{n-1}_{n'-n}(x)J^{n}_{n'-n}(x).
\end{aligned} \tag{D3}$$

APPENDIX E: ABSORPTION COEFFICIENTS

The absorption coefficients due to pair creation *in vacuo* are different for the two modes and are determined by the anti-Hermitian part of the vacuum response tensor. Without loss of generality, one may transform to the frame in which the photons are propagating across **B** ($k_z = 0$). The absorption coefficients then become

$$\begin{aligned}
\gamma_\parallel &= -\frac{8\pi i}{\omega_\parallel}R_E^{\parallel}e^{3*}_{\parallel}e^{3}_{\parallel}\alpha^{33(a)},\\
\gamma_\perp &= -\frac{8\pi i}{\omega_\perp}R_E^{\perp}e^{2*}_{\perp}e^{2}_{\perp}\alpha^{22(a)},
\end{aligned} \tag{E1}$$

$$\begin{aligned}
\alpha^{33(a)} &= i\Im\,\mathrm{reg}\alpha^{33} = -i\Im\alpha_2,\\
\alpha^{22(a)} &= i\Im\,\mathrm{reg}\alpha^{22} = -i\Im\alpha_1,
\end{aligned} \tag{E2}$$

in the approximation $N_{\perp,\parallel} = 1$, implying $k_\perp = \omega$, $k^2 = 0$, and hence $\alpha_0 = 0$, and $R_E^{\parallel} = R_E^{\perp} = \frac{1}{2}$. From (1) with (2), one has

$$\begin{aligned}
\Im\alpha_1 &= \frac{\omega^2}{k^2}\Im\alpha_0 - \frac{e^3B}{(2\pi)^2}\sum_{n',n}4p_{n'}p_nJ^{n-1}_{n'-n+1}J^{n}_{n'-n-1}\Im I^{(1)}_{nn'},\\
\Im\alpha_2 &= -\frac{\omega^2}{k^2}\Im\alpha_0 + \frac{e^3B}{(2\pi)^2}\frac{\omega^2}{k_z}\sum_{n',n}\Im I^{(2)}_{nn'}[(J^{n-1}_{n'-n})^2 + (J^{n}_{n'-n})^2],
\end{aligned} \tag{E3}$$

where from (C6), the imaginary parts are given by

$$\begin{aligned}
\Im I^{(a)}_{nn'} &= \frac{f'_{nn'}\pi}{\omega^2 g_{nn'}}, \qquad \Im I^{(b)}_{nn'} = \frac{f_{nn'}\pi}{\omega^2 g_{nn'}},\\
\Im I^{(1)}_{nn'} &= \Im I^{(a)}_{nn'} + \Im I^{(b)}_{nn'} = \frac{\pi}{\omega^2 g_{nn'}},\\
\Im I^{(2)}_{nn'} &= \frac{2k_z\pi}{\omega^2 g_{nn'}}(g^2_{nn'} - f_{nn'}f'_{nn'}),
\end{aligned}$$

with $f'_{nn'} = 1 - f_{nn'}$ and with $f_{nn'}$, $g_{nn'}$ given by (6) with $\omega' = \omega$. Using the identities in Appendix C, (E3) becomes

$$\begin{aligned}
\Im\alpha_1 &= -\frac{e^3B}{4\pi\omega^2}\sum_{n',n}\frac{1}{g_{nn'}}\left\{\left(\frac{\omega^2}{2} - (n+n')eB\right)[(J^{n-1}_{n'-n+1})^2\right.\\
&\quad \left. + (J^{n}_{n'-n-1})^2] + 4\sqrt{n'n}eBJ^{n-1}_{n'-n+1}J^{n}_{n'-n-1}\right\},\\
\Im\alpha_2 &= -\frac{e^3B}{4\pi\omega^2}\sum_{n',n}\frac{1}{g_{nn'}}\left\{\left(2m^2 + (n'+n)eB\right.\right.\\
&\quad \left.\left. + \frac{2(n-n')^2e^2B^2}{\omega^2}\right)[(J^{n-1}_{n'-n})^2 + (J^{n}_{n'-n})^2]\right.\\
&\quad \left. + 4\sqrt{n'n}eBJ^{n-1}_{n'-n}J^{n}_{n'-n}\right\}.
\end{aligned} \tag{E4}$$

which are equivalent to the expressions given by [11].

APPENDIX F: REGULARIZED α_i COMPONENTS

The second derivatives of the refractive indices with respect to frequency are given by

$$\begin{aligned}
\left.\frac{\partial^2 N_\perp}{\partial\omega^2}\right|_{\omega=0} &= \frac{\sin^2\theta}{(1+\gamma_0-\gamma_1\sin^2\theta)^2}\left\{\frac{(1+\gamma_0)\gamma_{11} - \gamma_1\gamma_{01}}{N_\perp}\right.\\
&\quad + N_\perp[(1+\gamma_0)(\gamma_{12}\sin^2\theta - \gamma_{11}\cos^2\theta)\\
&\quad \left. - \gamma_1(\gamma_{02}\sin^2\theta - \gamma_{01}\cos^2\theta)]\right\},\\
\left.\frac{\partial^2 N_\parallel}{\partial\omega^2}\right|_{\omega=0} &= \frac{\sin^2\theta}{(1+\gamma_0+\gamma_2\cos^2\theta)^2}\left\{\frac{(1+\gamma_0)\gamma_{21} - \gamma_2\gamma_{01}}{N_\parallel}\right.\\
&\quad + N_\parallel[(1+\gamma_0)(\gamma_{22}\sin^2\theta - \gamma_{21}\cos^2\theta)\\
&\quad \left. - \gamma_2(\gamma_{02}\sin^2\theta - \gamma_{01}\cos^2\theta)]\right\}.
\end{aligned} \tag{F1}$$

The forms of the γ_i and γ_{ij} are as follows

$$\gamma_0 = \frac{e^2}{\pi}\Big\{\frac{31}{9} - \frac{1}{2b} + \frac{1}{12b^2} - \frac{\ln(1+2b)}{2b} - \frac{\ln(1+6b)}{3} + \Big(\frac{7}{24}+2b\Big)\frac{1}{1+8b} - \Big(\frac{1}{12}+b\Big)\frac{1}{1+6b} - \Big(\frac{5}{24}+b\Big)\frac{1}{1+4b}$$
$$- \Big(4+\frac{3}{2b}\Big)\ln\frac{1+4b}{1+2b} - \Big(\frac{47}{12}+\frac{1}{3b}+\frac{1}{48b^3}\Big)\ln\frac{1+6b}{1+4b} - \Big(\frac{95}{12}+\frac{13}{6b}-\frac{1}{48b^3}\Big)\ln\frac{1+8b}{1+6b} - \frac{b}{360}\Big[\frac{6}{1+8b} - \frac{6}{1+4b} - \frac{(3+42b)}{(1+8b)^2}$$
$$+ \frac{12b}{(1+6b)^2} + \frac{(3+30b)}{(1+4b)^2} - 2b\Big(\frac{(5+24b)}{(1+4b)^3} + \frac{2(1+12b)}{(1+6b)^3} - \frac{(7+48b)}{(1+8b)^3}\Big)\Big]\Big\},$$

$$\gamma_1 = \gamma_0 - \frac{e^2}{\pi}\Big\{-\frac{103}{18} + \frac{1}{b} - \frac{1}{6b^2} - \frac{\ln(1+6b)}{3} + \frac{2b}{1+8b} + \frac{15b}{1+6b} + \frac{15b}{1+4b} + \frac{4b}{1+2b} + \frac{6b^2}{(1+6b)^2} - \Big(\frac{47}{12}+\frac{1}{8b^2}-\frac{1}{24b^3}\Big)$$
$$\times\ln\frac{1+6b}{1+4b} + \Big(\frac{95}{12}+\frac{1}{8b^2}+\frac{1}{24b^3}\Big)\ln\frac{1+8b}{1+6b} - 4\ln\frac{1+4b}{1+2b} - \frac{b}{60}\Big[\frac{1}{1+8b} - \frac{1}{1+4b} - \frac{7b}{(1+8b)^2} + \frac{2b}{(1+6b)^2} + \frac{5b}{(1+4b)^2}$$
$$+ \frac{16b^2}{(1+8b)^3} - \frac{8b^2}{(1+6b)^3} - \frac{8b^2}{(1+4b)^3} + \frac{4b}{(1+6b)^4}\Big]\Big\},$$

$$\gamma_2 = -\gamma_0 + \frac{e^2}{\pi}\Big\{\frac{b}{3} - \frac{\ln(1+6b)}{3} + \frac{2b}{3(1+2b)} + \frac{2b}{3(1+4b)} + \frac{b}{3(1+6b)} + \frac{b^2}{9(1+6b)^2} - \Big[\frac{2b^4}{45(1+6b)^4}\Big]\Big\},$$

$$\gamma_{01} = -\frac{e^2}{4\pi b}\Big\{-27 - \frac{31}{6b} + \frac{3}{4b^2} - \frac{1}{8b^3} + \Big(\frac{3}{2b^2}+\frac{2}{b}\Big)\ln(1+2b) + \Big(36+\frac{26}{b}+\frac{9}{2b^2}\Big)\ln\frac{1+4b}{1+2b} + \Big(\frac{287}{4}+\frac{23}{b}+\frac{7}{8b^2}+\frac{1}{32b^4}\Big)$$
$$\times\ln\frac{1+6b}{1+4b} - \Big(\frac{433}{4}+\frac{51}{b}+\frac{53}{8b^2}-\frac{1}{32b^4}\Big)\ln\frac{1+8b}{1+6b} - \Big(\frac{21}{24b}+\frac{73}{6}+42b\Big)\frac{1}{1+8b} + \Big(\frac{1}{4b}+6+27b\Big)\frac{1}{1+6b}$$
$$+ \Big(\frac{5}{8b}+\frac{37}{6}+15b\Big)\frac{1}{1+4b} + \frac{4b}{15} + \frac{1}{180}\Big[9\Big(\ln\frac{1+8b}{1+4b} + \frac{2+21b}{1+8b} - \frac{(2+15b)}{1+4b} - \frac{6b}{1+6b}\Big) + \frac{9}{2}\Big(-\frac{(1+28b+146b^2)}{(1+8b)^2}$$
$$+ \frac{1+20b+74b^2}{(1+4b)^2} + \frac{8b(1+9b)}{(1+6b)^2}\Big) - b\Big(-\frac{(21+292b+1008b^2)}{(1+8b)^3} + \frac{15+148b+360b^2}{(1+4b)^3} + \frac{6(1+24b+108b^2)}{(1+6b)^3}\Big)\Big]\Big\},$$

$$\gamma_{02} = \frac{e^2}{4\pi b}\Big\{-\frac{39}{4} + \frac{13}{8b} - \frac{3}{16b^2} + \frac{1}{32b^3} + \frac{1}{b}\ln(1+2b) - \frac{1}{4b}\ln(1+4b) + \Big(12+\frac{5}{b}\Big)\ln\frac{1+4b}{1+2b} + \Big(\frac{287}{12}+\frac{11}{3b}-\frac{1}{8b^2}-\frac{1}{96b^4}\Big)$$
$$\times\ln\frac{1+6b}{1+4b} - \Big(\frac{433}{12}+\frac{29}{3b}+\frac{1}{8b^2}+\frac{1}{96b^4}\Big)\ln\frac{1+8b}{1+6b} - \Big(6+\frac{9}{8b}\Big)\ln\frac{1+8b}{1+4b} + \Big(\frac{181}{24}+\frac{43}{24b}+\frac{1}{768b^4}\Big)\ln\frac{1+10b}{1+6b} - \Big(\frac{35}{24}+\frac{5}{12b}$$
$$- \frac{1}{768b^4}\Big)\ln\frac{1+6b}{1+2b} + \Big(-\frac{1}{12}+\frac{7b}{4}\Big)\frac{1}{1+2b} + \Big(\frac{13}{12}+9b\Big)\frac{1}{1+4b} + \Big(\frac{3}{4}+\frac{115b}{12}\Big)\frac{1}{1+6b} - \Big(\frac{25}{12}+14b\Big)\frac{1}{1+8b}$$
$$+ \Big(\frac{1}{3}+\frac{5b}{2}\Big)\frac{1}{1+10b} + \frac{b^2}{(1+6b)^2} + \frac{4b}{15} + \frac{1}{720}\Big[\frac{48b^3}{(1+6b)^4} + 12\ln\frac{1+8b}{1+4b} - \frac{3}{2}\ln\frac{1+10b}{1+2b} - \frac{3(1+24b)}{2(1+10b)} + \frac{12(1+21b)}{(1+8b)}$$
$$- \frac{54b}{(1+6b)} - \frac{12(1+15b)}{(1+4b)} + \frac{3(1+12b)}{2(1+2b)} + b\Big(\frac{3(4+47b)}{(1+10b)^2} - \frac{4(21+219b)}{(1+8b)^2} + \frac{18(1+18b)}{(1+6b)^2} + \frac{4(15+111b)}{(1+4b)^2} - \frac{3(2+11b)}{(1+2b)^2}\Big)$$
$$- 8b^2\Big(\frac{2(2+15b)}{(1+10b)^3} - \frac{(25+168b)}{(1+8b)^3} + \frac{9(1+9b)}{(1+6b)^3} + \frac{13+60b}{(1+4b)^3} - \frac{(1+3b)}{(1+2b)^3}\Big)\Big]\Big\},$$

$$\gamma_{11} = \gamma_{01} + \frac{e^2}{2\pi b}\Big\{\frac{2b}{15} - 8 + \frac{11}{9b} - \frac{1}{4b^2} + \frac{1}{24b^3} + 4\Big(3+\frac{1}{b}\Big)\ln\frac{1+4b}{1+2b} + \Big(\frac{287}{12}+\frac{47}{12b}+\frac{1}{8b^2}-\frac{1}{96b^4}\Big)\ln\frac{1+6b}{1+4b} - \Big(\frac{433}{12}+\frac{95}{12b}-\frac{1}{8b^2}$$
$$+ \frac{1}{96b^4}\Big)\ln\frac{1+8b}{1+6b} - \frac{2(1+7b)}{1+8b} + \frac{1+5b}{1+4b} + \Big(1+9b-\frac{1}{6b}\Big)\frac{1}{1+6b} + \Big(\frac{2b^2}{3}-6b^2\Big)\frac{1}{(1+6b)^2} - \frac{4b^2}{3(1+2b)^2} - \frac{16b^2}{3(1+4b)^2}$$
$$- \frac{4b^3}{(1+6b)^3} + \frac{1}{60}\Big[\ln\frac{1+8b}{1+4b} + \frac{8b^3(1-6b)}{3(1+6b)^5} + \frac{1+21b}{1+8b} - \frac{(1+15b)}{1+4b} - \frac{6b}{1+6b} - b\Big(\frac{7+73b}{(1+8b)^2} - \frac{(5+37b)}{(1+4b)^2} - \frac{2(1+18b)}{(1+6b)^2}\Big)$$
$$+ 8b^2\Big(\frac{2(1+7b)}{(1+8b)^3} - \frac{(1+5b)}{(1+4b)^3} - \frac{(1+9b)}{(1+6b)^3}\Big)\Big]\Big\},$$

$$\gamma_{12} = \gamma_{02} + \frac{e^2}{2\pi b}\Bigg\{-\frac{2b}{15} - \frac{27}{2} + \frac{9}{4b} - \frac{3}{8b^2} + \frac{1}{16b^3} - 8\ln\frac{1+4b}{1+2b} - \left(\frac{287}{18} + \frac{1}{12b^2} - \frac{1}{12b^3} + \frac{1}{48b^4}\right)\ln\frac{1+6b}{1+4b}$$
$$+ \left(\frac{433}{18} - \frac{1}{12b^2} - \frac{1}{12b^3} - \frac{1}{48b^4}\right)\ln\frac{1+8b}{1+6b} + 4\ln\frac{1+8b}{1+4b} + \left(-\frac{181}{36} + \frac{1}{24b^2} + \frac{1}{48b^3} + \frac{1}{384b^4}\right)\ln\frac{1+10b}{1+6b}$$
$$+ \left(\frac{35}{36} + \frac{1}{24b^2} - \frac{1}{48b^3} + \frac{1}{384b^4}\right)\ln\frac{1+6b}{1+2b} + \frac{25b}{6(1+2b)} + \frac{86b}{3(1+4b)} + \frac{81b}{2(1+6b)} + \frac{28b}{3(1+8b)} - \frac{5b}{3(1+10b)}$$
$$+ \frac{18b^2}{(1+6b)^2} + \frac{1}{720}\Bigg[\ln\frac{1+10b}{1+2b} - 8\ln\frac{1+8b}{1+4b} + \frac{24b}{(1+6b)^4} + 12b\left(\frac{2}{1+10b} - \frac{14}{1+8b} + \frac{3}{1+6b} + \frac{10}{1+4b} - \frac{1}{1+2b}\right)$$
$$- 4b^2\left(\frac{47}{2(1+10b)^2} - \frac{146}{(1+8b)^2} + \frac{74}{(1+4b)^2} + \frac{54}{(1+6b)^2} - \frac{11}{2(1+2b)^2}\right) + 16b^3\left(\frac{10}{(1+10b)^3} - \frac{56}{(1+8b)^3}\right.$$
$$\left.\left. + \frac{20}{(1+4b)^3} + \frac{27}{(1+6b)^3} - \frac{1}{(1+2b)^3}\right)\Bigg]\Bigg\},$$

$$\gamma_{21} = -\gamma_{01} + \frac{e^2}{15\pi}\left\{-1 + b + \frac{1}{1+6b} + \frac{2b}{(1+2b)^2} + \frac{2b}{(1+4b)^2} + \frac{b}{(1+6b)^2} + \frac{2b^2}{3(1+6b)^3} - \left[\frac{8b^4}{15(1+6b)^5}\right]\right\},$$

$$\gamma_{22} = -\gamma_{02} - \frac{e^2}{4\pi b}\Bigg\{-\frac{4b}{15} - 22 - \frac{25}{9b} + \frac{2b}{3} + \frac{1}{2b^2} - \frac{1}{12b^3} + \left(\frac{1}{b^2} + \frac{2}{b}\right)\ln(1+2b) + \left(24 + \frac{18}{b} + \frac{3}{b^2}\right)\ln\frac{1+4b}{1+2b}$$
$$+ \left(\frac{287}{6} + \frac{91}{6b} + \frac{5}{12b^2} + \frac{1}{48b^4}\right)\ln\frac{1+6b}{1+4b} - \left(\frac{433}{6} + \frac{211}{6b} + \frac{55}{12b^2} - \frac{1}{48b^4}\right)\ln\frac{1+8b}{1+6b} + \frac{8b}{3(1+2b)} - \frac{2b}{9(1+6b)^2}$$
$$+ \left(\frac{25}{6} + \frac{5}{12b} + \frac{46b}{3}\right)\frac{1}{1+4b} + \left(22b + 4 + \frac{1}{6b}\right)\frac{1}{1+6b} - \left(\frac{49}{6} + \frac{7}{12b} + 28b\right)\frac{1}{1+8b} + \frac{1}{180}\Bigg[\frac{16b^3}{(1+6b)^4}$$
$$+ 6\ln\frac{1+8b}{1+4b} + 6\left(\frac{2+21b}{1+8b} - \frac{(2+15b)}{1+4b} - \frac{6b}{1+6b}\right) - 3\left(\frac{1+28b+146b^2}{(1+8b)^2} - \frac{(1+20b+74b^2)}{(1+4b)^2} - \frac{8b(1+9b)}{(1+6b)^2}\right)$$
$$+ 2b\left(\frac{7+98b+336b^2}{(1+8b)^3} - \frac{5(1+10b+24b^2)}{(1+4b)^3} - \frac{2(1+24b+108b^2)}{(1+6b)^3}\right)\Bigg]\Bigg\}, \tag{F2}$$

with $b = B/B_{cr}$. The square bracket in each γ_i, γ_{ij} contains the third derivative contribution to the Euler-Maclaurin summation.

[1] V. Weisskopf, K. Dan. Vidensk. Selsk. Mat. Fys. Medd. **14**, Nr 6 (1936).
[2] W. Heisenberg and H. Euler, Z. Phys. **98**, 714 (1936).
[3] T. Erber, Rev. Mod. Phys. **38**, 626 (1966).
[4] W. Tsai and T. Erber, Phys. Rev. D **12**, 1132 (1975).
[5] J. Géhéniau, Physica (Amsterdam) **16**, 822 (1950).
[6] J. Géhéniau and M. Demeur, Physica (Amsterdam) **17**, 71 (1951).
[7] J. Schwinger, Phys. Rev. **82**, 664 (1951).
[8] D. B. Melrose and R. J. Stoneham, J. Phys. A **10**, 1211 (1977).
[9] J. S. Toll, Ph.D. thesis, Princeton University, 1952.
[10] N. P. Klepikov, Zh. Eksp. Teor. Fiz. **26**, 19 (1954).
[11] J. K. Daugherty and A. K. Harding, Astrophys. J. **273**, 761 (1983).
[12] S. L. Adler, Ann. Phys. (N.Y.) **67**, 599 (1971).
[13] J. S. Heyl and L. Hernquist, J. Phys. A **30**, 6485 (1997).
[14] J. I. Weise, M. G. Baring, and D. B. Melrose, Phys. Rev. D **57**, 5526 (1998); J. I. Weise, M. G. Baring, and D. B. Melrose, Phys. Rev. D **60**, 099901 (1999).
[15] P. A. Sturrock, Astrophys. J. **164**, 529 (1971).
[16] M. A. Ruderman and P. G. Sutherland, Astrophys. J. **196**, 51 (1975).
[17] J. Arons, Astrophys. J. **266**, 215 (1983).
[18] L. Mestel, *Stellar Magnetism* (Oxford University Press, New York, (1998).
[19] V. S. Beskin, Astrophysics (Engl. Transl.) **18**, 266 (1983).
[20] M. G. Baring and Alice K. Harding, Astrophys. J. **547**, 929 (2001).
[21] J. I. Weise and D. B. Melrose, Mon. Not. R. Astron. Soc. **329**, 115 (2002).
[22] C. Wilke and G. Wunner, Phys. Rev. D **55**, 997 (1997).
[23] M. V. Chistyakov, A. V. Kuznetsov, and N. V. Mikheev, Phys. Lett. B **434**, 67 (1998).
[24] V. N. Baier, A. I. Milstein and R. Zh. Shaisultanov, Phys. Rev. Lett. **77**, 1691 (1996).
[25] V. V. Usov and A. E. Shabad, Sov. Astron. Lett. **9**, 212 (1983).
[26] A. K. Harding, M. G. Baring, and P. L. Gonthier, Astrophys. J. **476**, 246 (1997).
[27] G. G. Pavlov and Yu. A. Shibanov, JETP Lett. **49**, 741 (1979).

[28] P. Mészáros and J. Ventura, Phys. Rev. D **19**, 3565 (1979).
[29] W. C. G. Ho and D. Lai, Mon. Not. R. Astron. Soc. **327**, 1081 (2001); W. C. G. Ho and D. Lai, Mon. Not. R. Astron. Soc. **338**, 233 (2003).
[30] F. Özel, Astrophys. J. **563**, 276 (2001); F. Özel, Astrophys. J. **583**, 402 (2003).
[31] D. B. Melrose and A. J. Parle, Aust. J. Phys. **36**, 799 (1983).
[32] A. E. Shabad, Ann. Phys. (N.Y.) **90**, 166 (1975).
[33] D. B. Melrose and R. J. Stoneham, Nuovo Cimento Soc. Ital. Fis. A **32**, 435 (1976).